Experimental investigation of Ferro-cement laminated masonry infilled in RC frame
Part 2: Evaluation of Failure Mode and Seismic Capacity under Lateral Load

Keywords
Masonry infill　　Ferro-cement
Strengthening　　Capacity evaluation

○ Debasish Sen*1　　Zasiah Tafheem *1
Md. Shafiul Islam *1　　Hamood Alwashali *2
Matsutaro Seki*3　　Masaki Maeda*4

1. Introduction:

Part 2 intends to analyze the experimental results i.e. failure modes, energy dissipation of Ferro-cement laminated masonry infill in RC frame from the experimental campaign presented in Part 1. This is followed by discussion on simplified evaluation procedure to predict lateral capacity of FC strengthened infill masonry in RC frame.

2. Failure mechanism:

2.1 Crack pattern and failure mode:

The final crack pattern of all the specimens are shown in Figure 1. In masonry infilled RC frame, long reinforcement of tension column yielded at above mid-height and upper critical section around 0.2% and 0.4% story drift. The hinge formation could be attributed to shear demand by sliding of infill masonry, as shown in Figure 1(a). Therefore, failure mechanism has been governed by the sliding of infill masonry with hinges on column. In specimen IM-FC-1, with 0.16% mesh reinforcement, initially several flexural cracks have been observed at the bottom of tension column where tensile reinforcement yielded at about 0.1% story drift. A clear separation of wall and bottom beam has also been observed. At the large story drift, direct punching shear failure of top of the tension column, as shown in Figure 1(b), has also been observed which has been confirmed by recorded strain values (>2000 μ) of the tie. Sliding at joint/interface of soffit and top of retrofitted infill have also been observed. Therefore, the specimen IM-FC-1 failed in shear following flexural yielding of tension column reinforcements i.e. peak resistance might be governed by flexure however post peak behavior has been governed by shear. In the specimen IM-FC-2, with 0.56% mesh reinforcement, no crack has been observed on the wall except at the bottom interface as shown in Figure 1(c). The longitudinal reinforcements of tension column experienced yielding at 0.1% story drift followed by a rupture at 2% story drift. Therefore, the IM-FC-2 the specimen showed rocking failure.

2.2 Component of story deformation:

Failure mode of structural wall, under lateral load, is mainly governed by shear, flexure or combination of the shear and flexure. To confirm the behavior, flexural and shear deformation in relation to the story deformation have been measured and are shown in Figure 2. In infilled masonry wall (IM), contribution of the flexural deformation is less than shear deformation throughout the courses of drift, as shown in Figure 2(a), which implies a shear dominated failure. In first retrofitted specimen IM-FC-1, flexural contribution is relatively more at lower story drifts as shown in Figure 2(b). At higher story drifts, tension column experienced direct punching shear failure which led to an increase in shear deformation. Another strengthened RC frame, namely IM-FC-2, experienced a flexure domination throughout course of the drift as shown in Figure 2(c). In other words, IM-FC-2 specimen acted like a flexural wall.

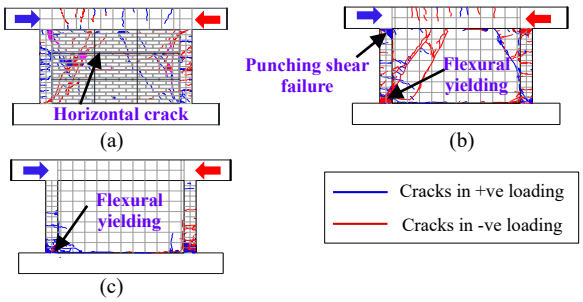

Figure 1: Crack pattern on (a) infilled masonry (IM), (b) IM-FC-1 and IM-FC-2 at 2% story drift

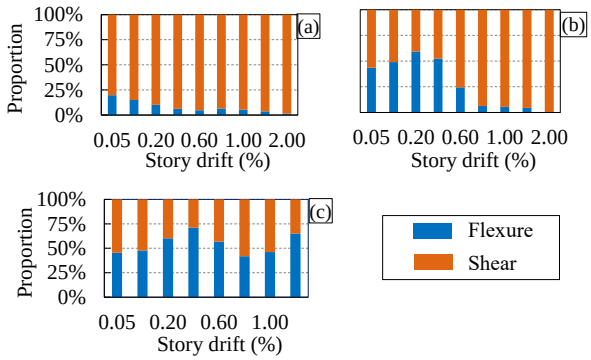

Figure 2: Contribution of shear and flexural components in story deformation of (a) IM, (b) IM-FC-1, and (c) IM-FC-2

3. Cumulative energy dissipation:

The cumulative dissipated energy by un-strengthened and strengthened masonry infill in RC frame has been computed using hysteresis loop area of lateral load-displacement curve and reported in Figure 3. The retrofitted specimen, IM-FC-1, showed almost two times energy dissipation than infilled masonry (IM). On the other hand, specimen IM-FC-2 showed almost similar energy

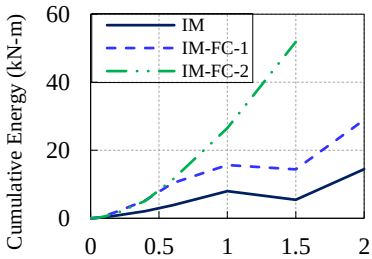

Figure 3: Energy dissipation at different drifts

dissipation trend as IM-FC-1 up to 0.6% drift which is followed by huge energy dissipation that indicates a ductile behavior. The more energy dissipation might be attributed to the flexure domination.

4. Evaluation of lateral capacity:

4.1 Interaction of shear and flexural capacity:

The interaction of shear and flexural capacity on the overall failure mechanism can be idealized as Figure 4, as suggested by ATC 32 [1] for RC column. The failure of specimen IM-FC-1 and IM- FC-2 can be assumed as failure mode B and C, respectively. To evaluate this phenomenon, the flexural strength and shear strength of retrofitted RC frame has been computed as per JBDPA 2001 [2].

Flexural shear capacity (Q_{fl})

The lateral capacity at flexural yielding, as shown in Figure 5(a), of the FC laminated masonry infill in RC frame has been computed using Eq. 1 and Eq. 2 as per JBDPA 2001, which is generally used for concrete wall.

$$Q_{fl} = {}^{M_u}/_{h_o} \quad (1)$$

$$M_u = a_t f_y l_w + 0.5\sum(a_{wv} f_{y,wm}).\, l_w + 0.5 N l_w \quad (2)$$

where, a_t = cross sectional area of column longitudinal reinforcement, f_y= yield strength of column longitudinal reinforcement, l_w = c/c distance of boundary columns, a_{wy}= area of vertical mesh reinforcement, $f_{y,wm}$ = yield strength of wire mesh, N=axial load on RC columns.

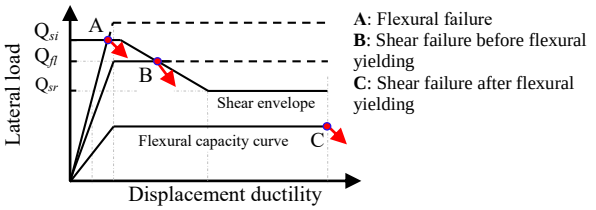

Figure 4: Interaction of flexure and shear capacity on failure

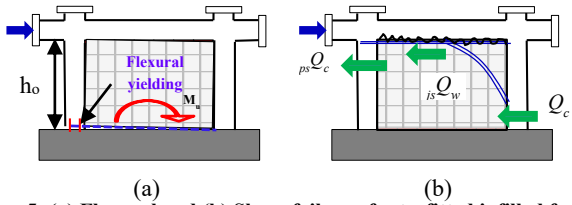

Figure 5: (a) Flexural and (b) Shear failure of retrofitted infilled frame

Shear Capacity (Q_s)

The schematic free body diagram of retrofitted masonry infilled RC frame after shear failure is shown in Figure 5(b), which actually occurred in specimen IM-FC-1 at higher story drifts. The total shear capacity (Q_s) can be evaluated by Eq. 3.

$$Q_s = {}_{ps}Q_c + {}_{js}Q_w + \alpha Q_c \quad (3)$$

The punching shear capacity (${}_{ps}Q_c$) of tension column, and lateral capacity of compression column (Q_c) (minimum of flexural (Q_{mu}) and shear capacity (Q_{mu})) of RC column can be computed as per JBDPA 2001[2]. The joint shear capacity (${}_{js}Q_w$) depends on the bond between interfaces. At initial stage, before any slippage at the interface of infill top and soffit, shear capacity has been considered as the shear strength of mortar at interface. After the occurrence of slippage wire mesh will be subjected to shearing force hence considered as the source of residual shear capacity at the interface. The initial and residual joint shear capacity can be evaluated from Eq. 4 and Eq. 5, respectively.

$${}_{js}Q_{wi} = \tau_{mor,mas} l_w t_{mas} + 2\tau_{mor,FC} l_w t_{mor,FC} \quad (4)$$

$${}_{js}Q_{wr} = \sum a_{wv}\, \tau_y \quad (5)$$

where, ${}_{js}Q_{wi}$ = initial shear capacity at joint, ${}_{js}Q_{wr}$ = residual shear capacity at joint, $\tau_{mor,mas}$/ $\tau_{mor,FC}$ = shear strength of mortar in masonry joint and Ferro-cement (compressive strength/20), t_{mas}/ t_{FC} = thickness of masonry wall and FC layer, $\tau_{y,wm}$ =shear strength of wire mesh ($f_{y,wm}/\sqrt{3}$).

4.2 Verification of seismic capacity:

All of the computed capacity values are reported in Table 1. The envelop curve of specimen IM-FC-1 and IM-FC-2 with the prediction values are shown in Figure 6 (a)-(b). It is evident that the flexural capacity without considering wire mesh could give fair approximation of lateral load capacity of FC retrofitted masonry infilled RC frame. This might be attributed to the fact that all the wire did not face stretch except those have been directly connected to the bottom beam through bolt and steel plate.

The post peak response of specimen IM-FC-1 has been governed by the punching shear of tension column hence the residual shear capacity can be evaluated using Eq. 3. The plot on Figure 6(a) shows that the proposed estimation method gave a very conservative estimation of residual shear resistance which could be attributed to the friction at the interface which has not been considered.

Table 1: Lateral capacity of specimens

Lateral capacity (kN)		Specimen	
		IM-FC-1	IM-FC-2
Experimental	Peak (avg.)	534	588
	Residual (avg.)	373	-
Flexural capacity, Q_{fl} (w/ wire mesh)		585	741
Flexural capacity, Q_{fl} (w/o wire mesh)		509	509
Initial shear capacity, Q_{si}		824	867
Residual shear capacity, Q_{sr}		254	408

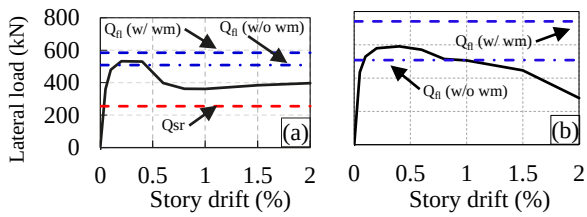

Figure 6: Envelop load-story drift curve of (a) IM-FC-1 and IM-FC-2

5. Conclusions:

1. Ferro-cement lamination on infilled masonry showed improvement of lateral strength and energy dissipation.
2. The lateral capacity could be predicted by the proposed evaluation method.

ACKNOWLEDGMENT

This research is supported by SATREPS project lead by Prof. Nakano Yoshiaki, U. Tokyo and JSPS KAKENHI Grant Number JP18H01578 (Principal investigator: Prof. Masaki Maeda, Tohoku University). This work is also supported by JST Program on OPERA project.

REFERENCES

1) Nutt, R. V. (1996). Improved seismic design criteria for California bridges: provisional recommendations (No. ATC-32, Final Report).

2) Japan Building Disaster Prevention Association, Standard for seismic evaluation of existing concrete Buildings, 2001

1*東北大学大学院　大学院生　（工学）
2*東北大学大学院　助教・博士（工学）
3*建築研究所　特別客員研究員・博士（工学）
4*東北大学大学院研究科　教授・博士（工学）

1*Graduate School of Engineering, Graduate student, Tohoku Univ.
2* Asst. Prof, Graduate School of Engineering, Tohoku University, Dr..Eng
3* Visiting Research Fellow, Building Research Institute, Dr.Eng
4* Professor, Graduate School of Engineering, Tohoku University, Dr..Eng